Turning-ray tomography and tomostatics

Babatunde Arenrin, Gary Margrave, and John Bancroft

ABSTRACT

Turning-ray tomography is a good tool for estimating near surface velocity structure, especially in areas where conventional refraction statics fail such as in the case of a hidden layer. The velocity model from turning-ray tomography can be used for static correction, wave equation datuming and prestack depth migration. In this research we apply turning-ray tomography to the statics problem of the Hussar 2D seismic line. This process is referred to as tomostatics. The traveltime tomography algorithm is similar to the constrained damped simultaneous iterative reconstruction technique (cdSIRT). The two-point problem for ray-tracing interpolation was used for forward modelling. To verify results from tomostatics, we compared datasets after tomostatics with datasets using the delay-time approach of a conventional refraction statics. The inversion result converged after 50 iterations and was used for statics correction. This inverted velocity model is reliable to a depth of about 750 meters, i.e. from the surface location to about one-fifth of the farthest offset (the recommended depth of sounding for turning rays). Our results show that the velocity model from turning-ray tomography reveals a hidden, slow velocity layer between two fast velocity layers that conventional refraction statics would not detect. The hidden layer is in agreement with the interval velocities from well logs. As we would expect, the stacked section, after applying tomostatics, shows better continuity of events compared to the stacked section from conventional refraction statics.

INTRODUCTION

Seismic tomography is applicable to a wide range of problems in the oil industry, ranging from exploration to production. Tomography can be applied to seismic data in order to estimate near-surface velocity structure in areas where refraction statics techniques fail due to poor data or the absence of a smooth refractor structure (Stefani, 1995). Seismic tomography exists in two forms: traveltime tomography and diffraction tomography. Traveltime tomography is applicable when the target's size is much larger than the seismic wavelength. This approach is based on the high frequency assumption of ray theory (Woodward, 1989) and can be implemented using reflection traveltimes or first arrivals (refraction) traveltimes. Diffraction tomography on the other hand should be the form of choice if the size of target is comparable to the seismic wavelength because the propagation of seismic waves is modelled as scattered energy using diffraction theory (Lo and Inderwiesen, 1994). In diffraction tomography, the wavefields are back propagated through the medium similar to reverse time migration.

Traveltime tomography involves the integrals of reflection or first arrival traveltimes over their raypaths. The mathematical expression for the traveltime is given in (1) as

$$t_i = \sum_j d_{ij}/v_j = \sum_j d_{ij}s_j, \tag{1}$$

where t_i is the total travel time along the ith ray-path, d_{ij} is the path length in the jth cell of the velocity model for the ith ray, v_j is the velocity in the jth cell and s_j is the slowness in the jth cell (Jones, 2009).

The travel time equation can be re-written in matrix notation as

$$\vec{T} = \mathbf{D}\vec{S}, \tag{2}$$

where $\mathbf{D}$ is the matrix of the lengths of the rays (path length), $\vec{S}$ is the slowness vector and $\vec{T}$ is the observed traveltime vector. We can solve for the slowness vector $\vec{S}$ using least squares inversion. The least squares solution to (2) is given as

$$\vec{S} = \left(\mathbf{D}^T\mathbf{D}\right)^{-1}\mathbf{D}^T\vec{T}. \tag{3}$$

The Eikonal solution to the wave equation

In order to understand traveltime tomography and its assumptions and/or limitations, we show the derivation of the Eikonal solution to the wave equation after Yilmaz (2001). This solution often expressed as first order partial derivatives of traveltimes with respect to the space coordinates has proved useful in the way we formulate the forward modelling engine.

Suppose we consider a compressional wave in three dimensions with its analytical form represented as

$$P(x, y, z; t) = P_0 \exp(-i\omega t + ik_x x + ik_y y + ik_z z), \tag{4}$$

and the three dimensional scalar wave equation expressed as

$$\frac{\partial^2 P}{\partial x^2} + \frac{\partial^2 P}{\partial y^2} + \frac{\partial^2 P}{\partial z^2} = \frac{1}{v^2}\frac{\partial^2 P}{\partial t^2}, \tag{5}$$

we can compute the partial derivatives of (4) and substitute the result into (5) to derive the dispersion relation of the scalar wave equation in (6), given as

$$k_x^2 + k_y^2 + k_z^2 = \frac{\omega^2}{v^2}, \tag{6}$$

where P_0 is the wave amplitude, t is the traveltime, k_x, k_y, k_z, ω are the Fourier duals of the space and time variables x, y, z, t respectively, and v is the propagation velocity of the compressional plane wave.

The phase term in equation (4) can be re-written in the form

$$P(x, y, z; t) = P_0 \exp\{-i\omega[t - (\frac{k_x}{\omega}x + \frac{k_y}{\omega}y + \frac{k_z}{\omega}z)]\}, \qquad (7)$$

from which a three dimensional traveltime surface can be defined as

$$T(x, y, z) = \frac{k_x}{\omega}x + \frac{k_y}{\omega}y + \frac{k_z}{\omega}z. \qquad (8)$$

The traveltime surface $T(x, y, z)$ is replaced in (7), and the wavefield expression takes the form

$$P(x, y, z; t) = P_0 \exp\{-i\omega[t - T(x, y, z)]\}. \qquad (9)$$

In order to verify that the form in (9) satisfies the scalar wave equation, (9) is differentiated twice with respect to the space and time coordinates and the results are replaced in to the wave equation in (5). (10), (11), (12), and (13) are the second order partial derivatives of the space and time variables.

$$\frac{\partial^2 P}{\partial x^2} = -P_0 \left[\omega^2 \left(\frac{\partial T}{\partial x} \right)^2 - i\omega \frac{\partial^2 T}{\partial x^2} \right] \exp\{-i\omega[t - T(x, y, z)]\}, \qquad (10)$$

$$\frac{\partial^2 P}{\partial y^2} = -P_0 \left[\omega^2 \left(\frac{\partial T}{\partial y} \right)^2 - i\omega \frac{\partial^2 T}{\partial y^2} \right] \exp\{-i\omega[t - T(x, y, z)]\}, \qquad (11)$$

$$\frac{\partial^2 P}{\partial z^2} = -P_0 \left[\omega^2 \left(\frac{\partial T}{\partial z} \right)^2 - i\omega \frac{\partial^2 T}{\partial z^2} \right] \exp\{-i\omega[t - T(x, y, z)]\}, \qquad (12)$$

$$\frac{\partial^2 P}{\partial t^2} = -P_0 \omega^2 \exp\{-i\omega[t - T(x, y, z)]\}. \qquad (13)$$

Substituting these partial derivatives into the wave equation, the wave equation takes the form in (14),

$$\omega^2 \left[\left(\frac{\partial T}{\partial x} \right)^2 + \left(\frac{\partial T}{\partial y} \right)^2 + \left(\frac{\partial T}{\partial z} \right)^2 \right] - i\omega \left(\frac{\partial^2 T}{\partial x^2} + \frac{\partial^2 T}{\partial y^2} + \frac{\partial^2 T}{\partial z^2} \right) = \frac{\omega^2}{v^2(x, y, z)}, \qquad (14)$$

with the terms on the left having both real and complex values. Notice that the term on the right is real valued. In order that the terms on the left contain only real values, the imaginary term needs to vanish.

Re-writing (14) to include only the real valued terms, we obtain the relation in (15)

$$\left(\frac{\partial T}{\partial x}\right)^2 + \left(\frac{\partial T}{\partial y}\right)^2 + \left(\frac{\partial T}{\partial z}\right)^2 = \frac{1}{v^2(x,y,z)}. \tag{15}$$

The expression in (15) is the Eikonal solution to the scalar wave equation. It gives the traveltime $T(x,y,z)$ for a ray passing through a point (x,y,z) in a medium with velocity $v(x,y,z)$. The eikonal solution in (15) is derived from a plane wave with constant amplitude P_0.

A similar expression for the Eikonal solution to the wave equation can be derived for a plane wave whose amplitude varies with position. The analytical form of such a plane wave takes the form

$$P(x,y,z;t) = P_0(x,y,z)\exp\{-i\omega[t - T(x,y,z)]\}, \tag{16}$$

and the Eikonal solution is given by

$$\left[\left(\frac{\partial T}{\partial x}\right)^2 + \left(\frac{\partial T}{\partial y}\right)^2 + \left(\frac{\partial T}{\partial z}\right)^2\right] - \frac{1}{\omega^2 P_0}\left(\frac{\partial^2 P_0}{\partial x^2} + \frac{\partial^2 P_0}{\partial y^2} + \frac{\partial^2 P_0}{\partial z^2}\right) = \frac{1}{v^2(x,y,z)}, \tag{17}$$

comparing (15) with (17), the two expressions are equivalent if and only if the second term on the left side of (17) vanishes. The condition for this for arbitrary amplitude variations is that the temporal frequency tends to infinity ($\omega \to \infty$, i.e. $1/\omega \to 0$). If we make this assumption, then (15) and (17) are equivalent.

This is the high frequency assumption. The Eikonal solution to the wave equation is a good approximation in the high frequency limit. The theory of traveltime tomography is based on the Eikonal solution to the wave equation.

Series expansion methods in traveltime tomography

Generally, there are two types of image reconstruction techniques in traveltime tomography. These are the series expansion methods and the transform methods (Lo and Inderwiesen, 1994). The series expansion methods allow for curved raypath trajectories through the target area and are well suited for traveltime tomography. The transform methods on the other hand allow only straight raypath trajectories through the target medium and are used in the field of medical sciences. In this paper we will limit our discussions to the series expansion methods of traveltime tomography.

Similar to inversion procedures, the series expansion method begins with an initial or starting model. The starting model is updated during each iteration until it converges to the best solution. The forward modelling engine can be a finite difference algorithm or a ray tracing algorithm for predicting traveltimes. A ray tracing algorithm traces ray through a starting model and computes predicted travel times using (1). The tomography

must then iterate to try to converge to the best estimate of the true model by minimizing the differences between the observed and predicted travel times (Jones, 2009).

Kaczmarz' approach to traveltime tomography

The Kaczmarz' approach is a series expansion method that can be implemented in two ways, viz: the algebraic reconstruction technique (ART) and the simultaneous iterative reconstruction technique (SIRT).

In order to illustrate traveltime tomography, we present a schematic of a ray tracer through a gridded slowness model in Figure (1). The ray tracer shoots rays from the source to the receiver as depicted below.
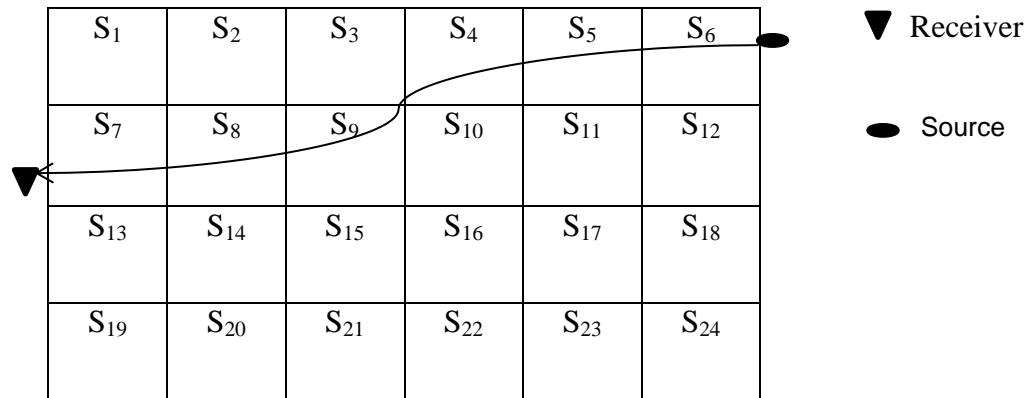
FIG. 1. A schematic of a ray tracer.

The Kaczmarz's approach uses a discrete model function such as $S_i, i = 1, 2..., 24$, which are the cells in Figure (1). The total traveltime for a ray travelling from the source to the receiver is the sum of the individual traveltimes in each cell traversed by the ray. Notice that the ray-path traversed cells S6, S5, S4, S9, S8, and S7 in the direction of the arrow. The schematic above is a simple illustration for a single source and receiver configuration, by adding more sources and receivers to the figure above, it is possible that all the cells will be traversed by at least one single ray-path.

However in reality, many of the elements of the matrix of the length of rays (matrix **D** from (1)), will be zero (Jones, 2009) because not all the cells will be traversed by rays. The slowness vector is solved using by tracing rays through a starting model to obtain predicted traveltimes. The predicted traveltimes are subtracted from the observed traveltimes (the observed traveltimes can be picked by an auto-picker). The absolute difference or data residual is used in (3) to update the starting model. This process of tracing rays and data subtraction is repeated until the data difference converges to a pre-defined or specified tolerance (Lo and Inderwiesen, 1994).

To illustrate how the inverse problem is solved in traveltime tomography, we consider a simple case of two rays traversing a two-cell model (Lo and Inderwiesen, 1994), i.e. each of the rays d_{1j} and d_{2j} traverse each slowness cell $S_i, i = 1, 2$. Thus applying (1), an

expression for the traveltimes in terms of the path lengths and slowness vectors can be represented as

$$t_1 = d_{11}s_1 + d_{12}s_2$$
$$t_2 = d_{21}s_1 + d_{22}s_2, \tag{18}$$

where $t_i, i = 1, 2$ is the traveltime corresponding to each ray. In order to solve (18) the ray tracing algorithm shoots rays through an estimate of the slowness cells s_1 and s_2 to obtain predicted travel times. At each iteration step, the data residuals are used to update the slowness cells by solving the least squares inversion in (2) until a good match between the predicted and the observed traveltimes is obtained.

Algebraic reconstruction technique (ART) and simultaneous iterative reconstruction technique (SIRT)

As mentioned in the previous section, the ART and SIRT techniques are two implementations of the Kaczmarz' method. The two methods are quite similar, however one major difference between ART and SIRT is that in ART the ray tracer shoots one ray at a time through the starting model, and the model is updated using (19). In SIRT the ray tracer shoots as many rays as possible through the starting model and the model update given in (20) is a weighted form of (19).

Lo and Inderwiesen (1994) showed that for the ART technique the correction or update, Δs_j applied to the starting model can be expressed as

$$\Delta s_j = d_{ij} \frac{\left| t_i^{observed} - t_i^{predicted} \right|}{\sum_j (d_{ij})^2}. \tag{19}$$

This is the update recommended by the ith ray to all j cells.

Lo and Inderwiesen (1994) also showed that for the SIRT technique the update Δs_j applied to the starting model is given as

$$\Delta s_j = \frac{1}{W_j} \sum_{i=1}^{I} d_{ij} \frac{\left| t_i^{observed} - t_i^{predicted} \right|}{\sum_j (d_{ij})^2}, \tag{20}$$

where W_j is the number of rays intersecting the jth cell or some other suitable ray density weight used to obtain an average correction Δs_j, and I is the total number of rays. The SIRT process is equivalent to tracing all rays through the model so that all Δs_j corrections for all the rays are known.

Turning-ray tomography and tomostatics

Turning-ray tomography is an inversion technique that employs turning rays from conventional surface acquisition geometry to iteratively solve for velocity in the near surface between sources and receivers (Stefani, 1995). The depth of sounding of turning rays is on the order of one-fifth the source-receiver offset provided the overall velocity field allows sufficient ray bending to return to the surface (Zhu et al, 1992). Tomostatics stands for turning-ray tomography followed by statics corrections (Zhu, et al., 1992).

Applications of turning-ray tomography and tomostatics are being evolved from statics correction to wave-equation datuming or prestack depth migration (Zhu, 2002). Tomostatics have advantages when compared to refraction statics especially in regions where no refractors can be easily identified, in regions where high velocity materials overlay low velocity sediments immediately below the topography commonly referred to as a hidden layer in refraction statics, or the lack of smooth velocity structure such that conventional refraction statics usually fail due to continuously refracted rays (Zhu, 2002; Stefani, 1993).

It is worth mentioning that one of the advantages of turning-ray tomography over reflection traveltime tomography is that the ambiguities between reflection depth and velocity in reflection traveltime tomography are absent in turning-ray tomography (Stefani, 1995).

The work presented here focuses on the application of turning-ray tomography to the statics problem. The motivation for this work is its similarity to full waveform inversion. The velocity model from turning-ray tomography can be used as a starting model for full waveform inversion. The success of full waveform inversion is dependent on how close the starting model is to the global solution. A way of obtaining such starting model is by traveltime tomography (Pratt and Shipp, 1999).

The data for this work is a 2D seismic line from Hussar, central Alberta and it is about 4.5km long running from Southwest to Northeast. The seismic source is dynamite with shot spacing of 20m and a total of 269 shot points. The number of receivers is 448 with receiver spacing of 10m.

Zhu (2002) gave some key steps and quality controls to run tomostatics in order to ensure the stability of the solution. Some of the key steps are: picking the first arrivals consistently for turning-ray tomography, removing any previously applied elevation and velocity statics before tomostatics, and repicking nmo velocities after tomostatics. The quality control methods are: observing the picked first arrivals, checking the ray density map for good ray coverage, fitting first arrival, and observing the continuity of reflectors on stack responses.

Forward modelling/ray tracing and inversion

After geometry assignment, we picked firstbreaks on the shot gathers, with the assumption that the firstbreaks observed on the seismic data are as a result of turning or continuously refracted arrivals. The initial velocity model for turning-ray tomography was 4480 meters wide and 1000 meters deep and was digitized into rectangular cells of

10m by 10m. The ray tracer for the forward model is described by Langan et al, (1984) two-point problem (see appendix A). Rays were traced through the model to obtain predicted traveltimes. The traveltime residuals were used to derive velocity updates (Bell et al, 1994) using equation (20) till the stopping criterion was reached. Stopping criteria are defined by Dennis and Schnabel (1983). The stopping criterion was the point at which the decrease in the traveltime residual was negligible. This occurred at the 50th iteration.

The inverse problem was constrained by choosing the minimum eigenvalue to invert and the maximum residual traveltime to use in the inversion. This approach is quite similar to the constrained damped SIRT (cDSIRT) described by Zhu et al, (1992). The inversion program solves (20) directly and updates the starting model with the assumption that the matrix **D** of the lengths of rays do not change significantly.

Field data examples

Figure 2 below shows a raw shot gather from Hussar, showing the first arrivals before (left) and after firstbreaks picking (right). The shot gather reveals the area has significant statics problem that need to be resolved.
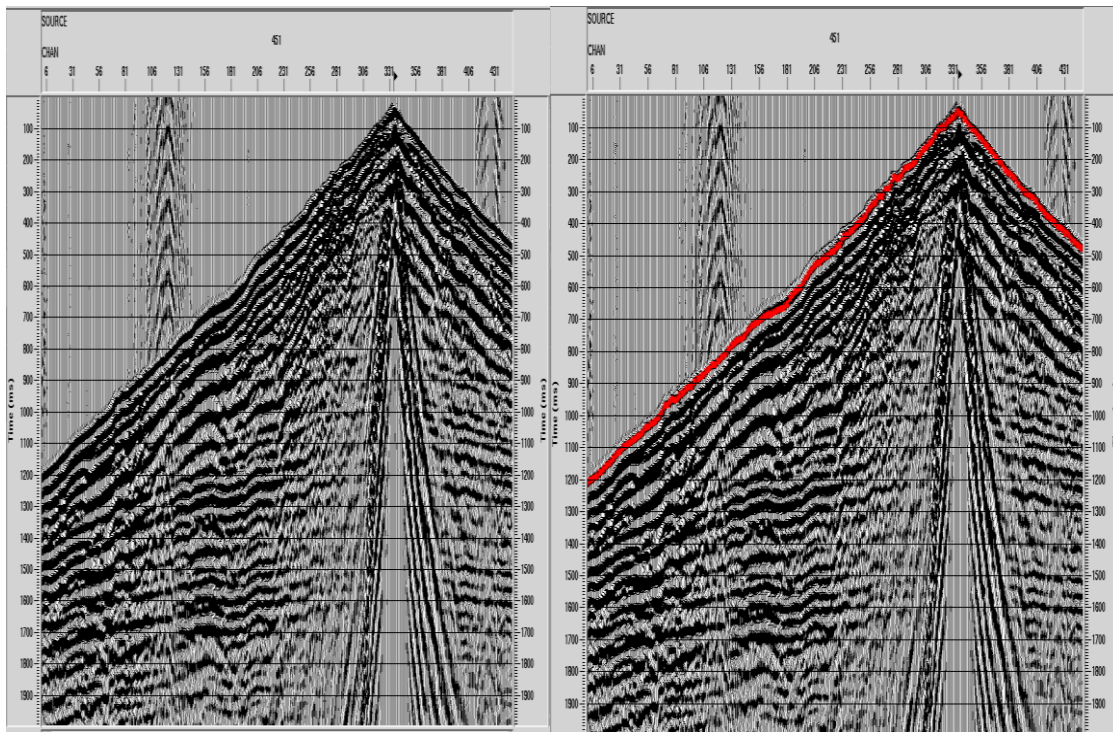
FIG. 2. Shot gather before (left) and after firstbreaks picks (right). Firstbreaks picks are in red.

Prior to inversion, no significant processing was performed on the data before inversion other than surface noise attenuation and filtering before and after stacking to get rid of low frequency coherent noise.

The ray density map of rays were traced through the velocity model is shown in Figure 3 below. It is evident that there is better ray coverage between 100-600 meters. This

suggests that in this area below the surface, the velocity model from turning-ray tomography is more reliable because more rays have traversed the cells. Areas without good ray coverage will produce artefacts in the final solution.

Shown in Figure 4 is the starting model for inversion obtained from refraction statics. The starting model converged to the best solution After 50 iterations. Figure 5 shows the final velocity model after convergence. The final velocity model was used to correct for statics.
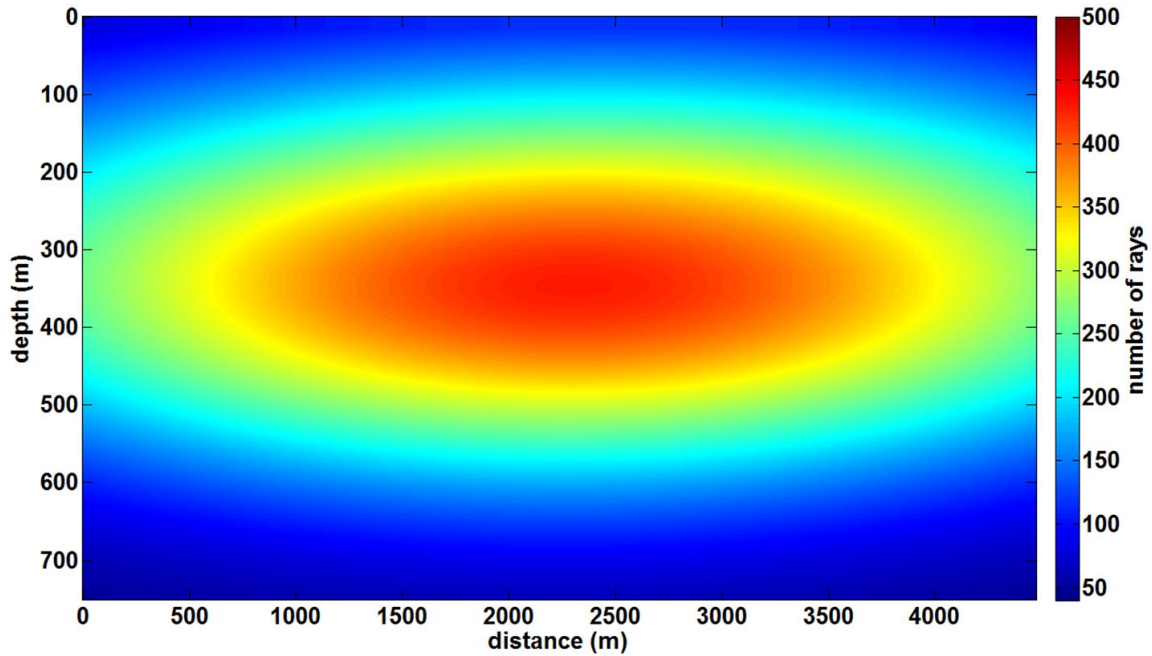
FIG. 3. Ray density for turning-ray tomography after damping.
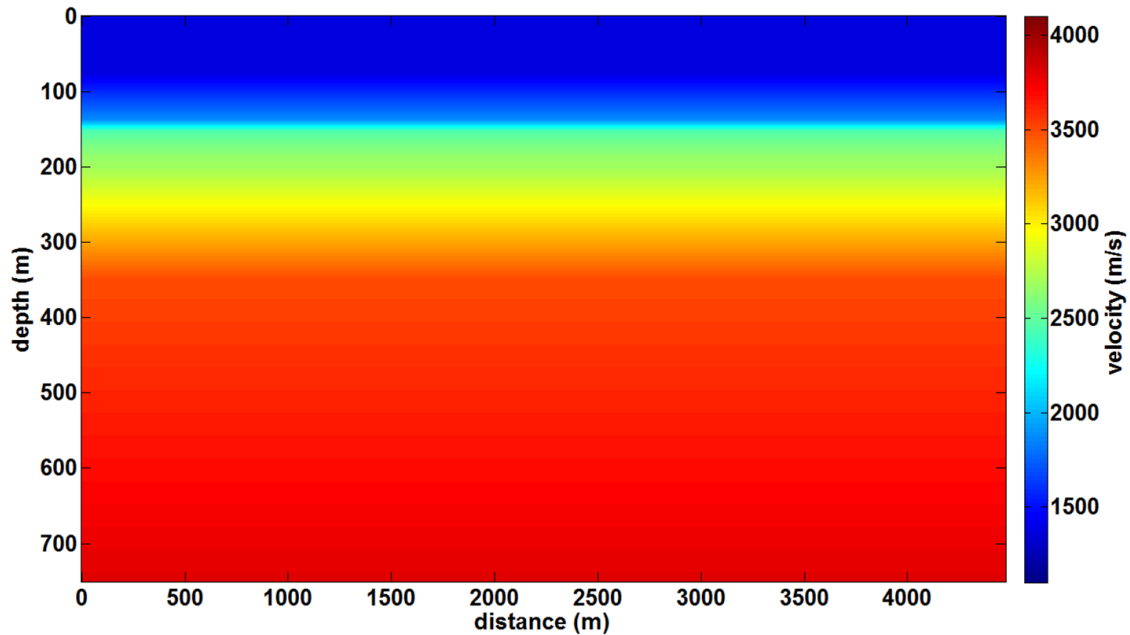
FIG. 4. Initial velocity model for turning-ray tomography.
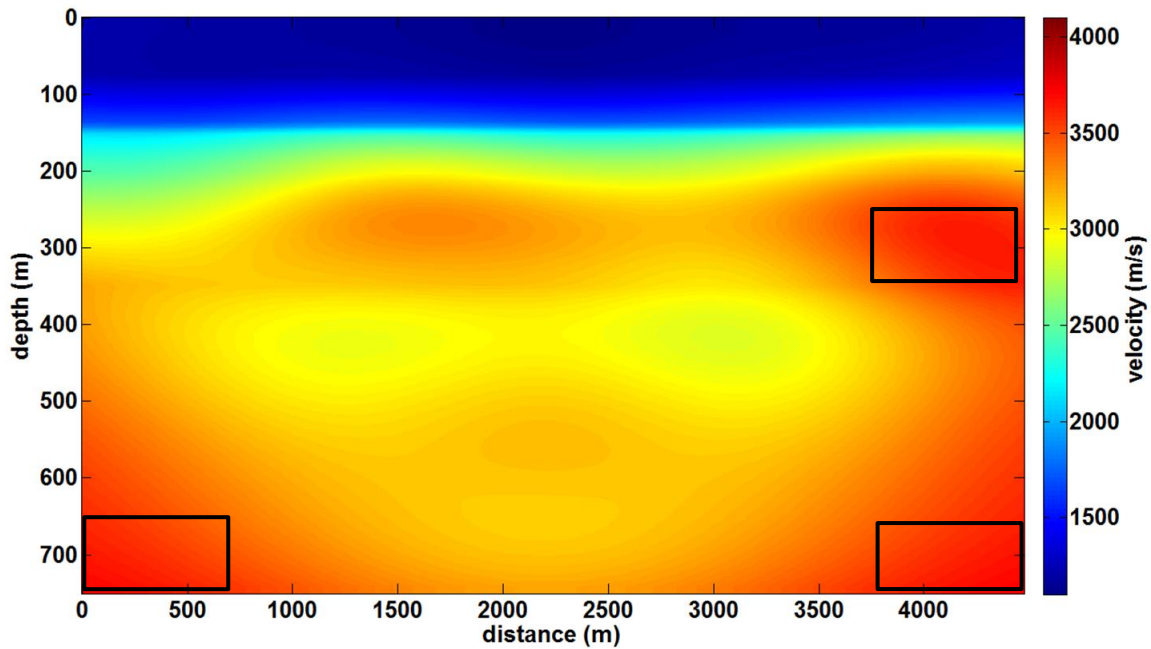
FIG. 5. Final velocity model after 50 iterations. The black boxes show edge effects due to poor ray coverage.
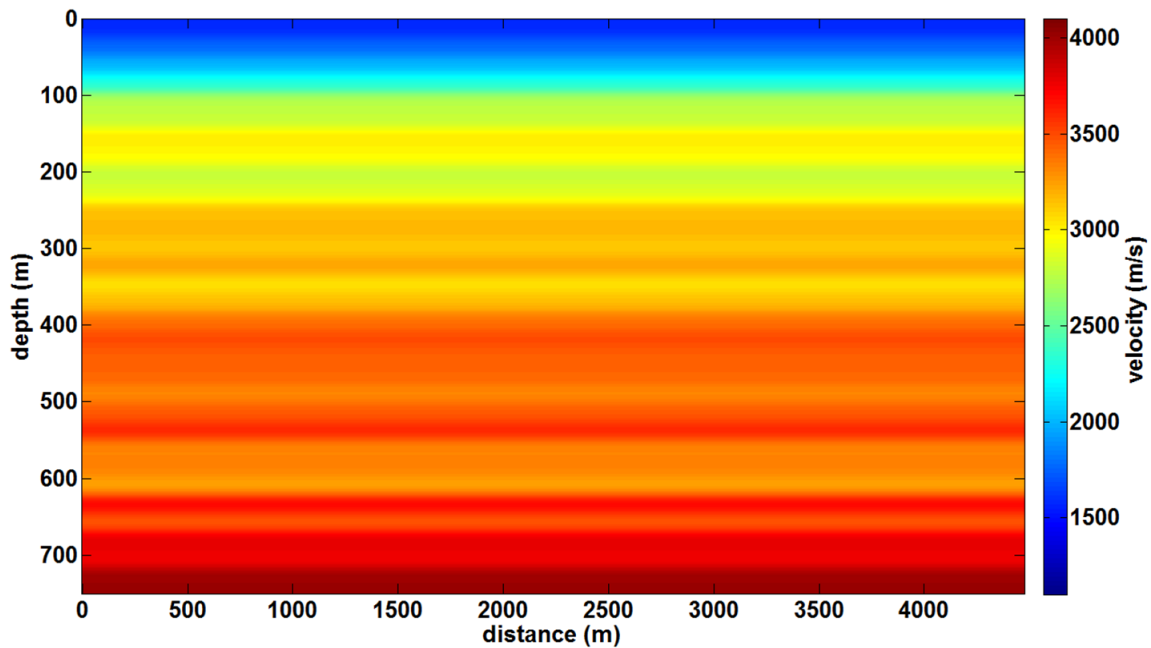
FIG. 6. Smoothed well velocities. Smoother Length is 200 meters.

The final velocity model shown in Figure 5 is in agreement with the smoothed well velocities shown in Figure 6 (length of smoother is 200 meters). The well that intersects the seismic line was logged from a depth of 1570 meters to 200 meters. From 200 meters to the surface where was no log data, the well velocities were interpolated between 2700 m/s and 1500 m/s. The final velocity model from turning-ray tomography and the smoothed well velocities reveal a hidden layer. The hidden layer from the tomogram is

between 350 and 450 meters, and between 350 and 400 meters from the smoothed well velocities. An explanation for this shift could be due to tying challenges associated with seismic and well logs.

The velocity model from tomography was used to create synthetic shot records using an acoustic finite difference algorithm as shown in Figure 7. The observed firstbreaks were superimposed on the synthetic shot record in Figure 7 (right). The predicted firstbreaks and the observed firstbreaks fit well.
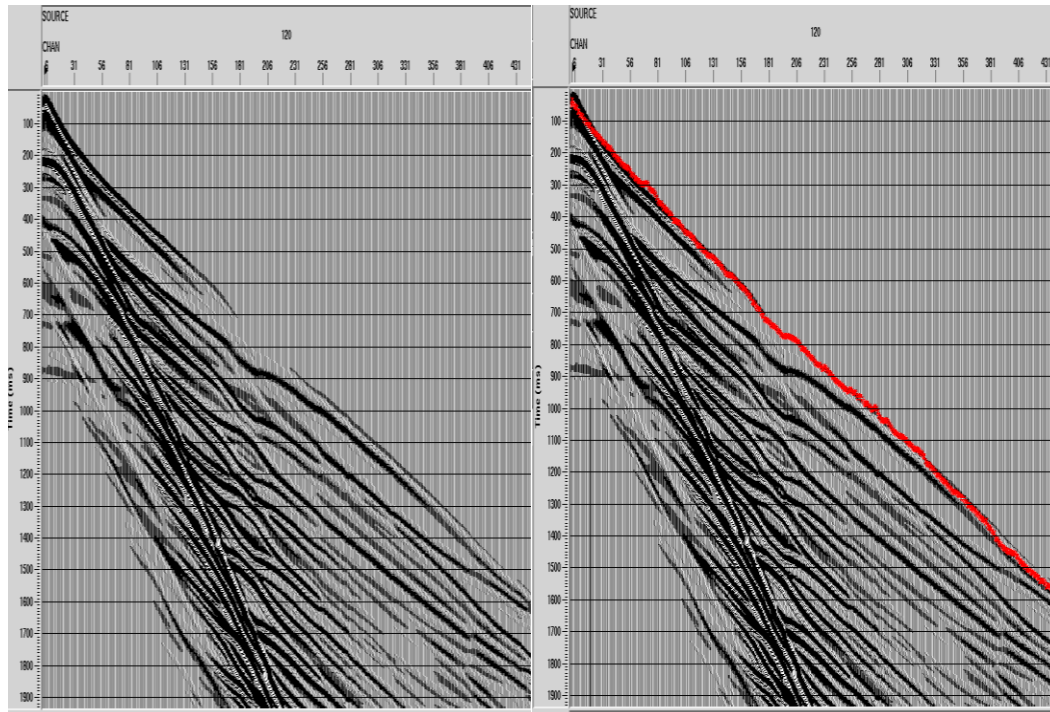
FIG. 7. Synthetic shot record using final velocity model from tomography**.**

We corrected for statics using conventional refraction method in order to compare the results with tomostatics. The stacked section after conventional refraction statics and tomostatics are shown in Figures 8 and 9 respectively. The reflection event at about 1200 milliseconds on the stacked section after tomostatics (red box) has been improved in terms of continuity and the structure of the event. The later remark is of great importance to seismic interpreters. The interpretation of the event in the red box in Figure 8 as a channel fill sediment will be incorrect and will lead errors in interpretation.
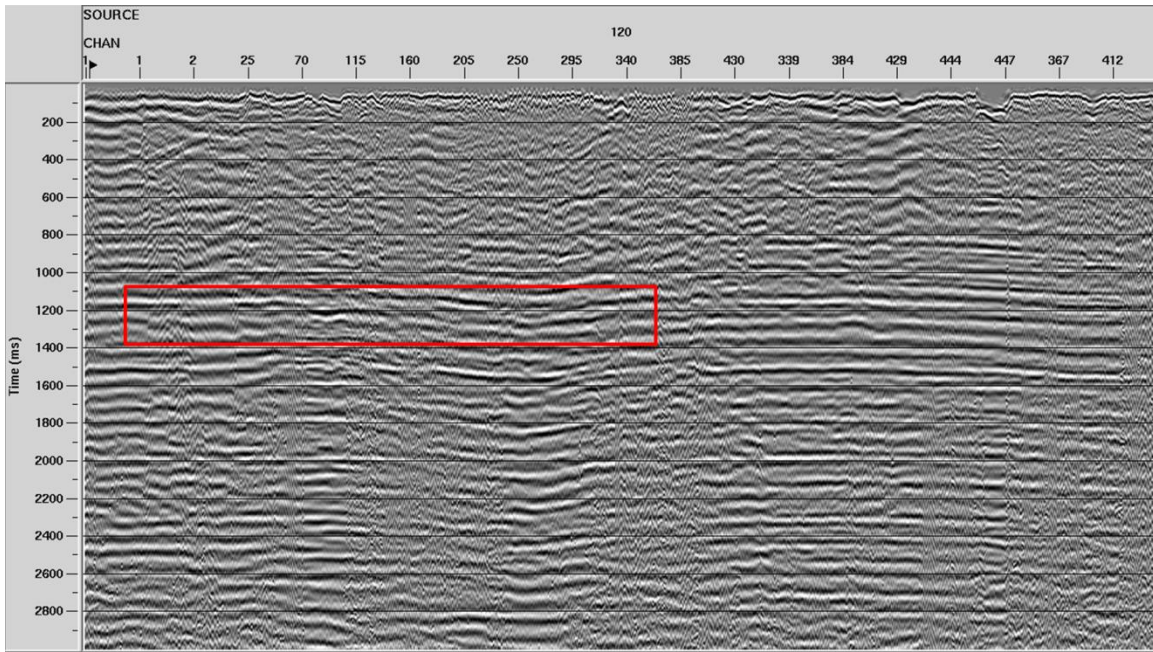
FIG. 8. Stacked section after conventional refraction statics. The structure at 1200ms (red box) is not real and it is due to unresolved statics.
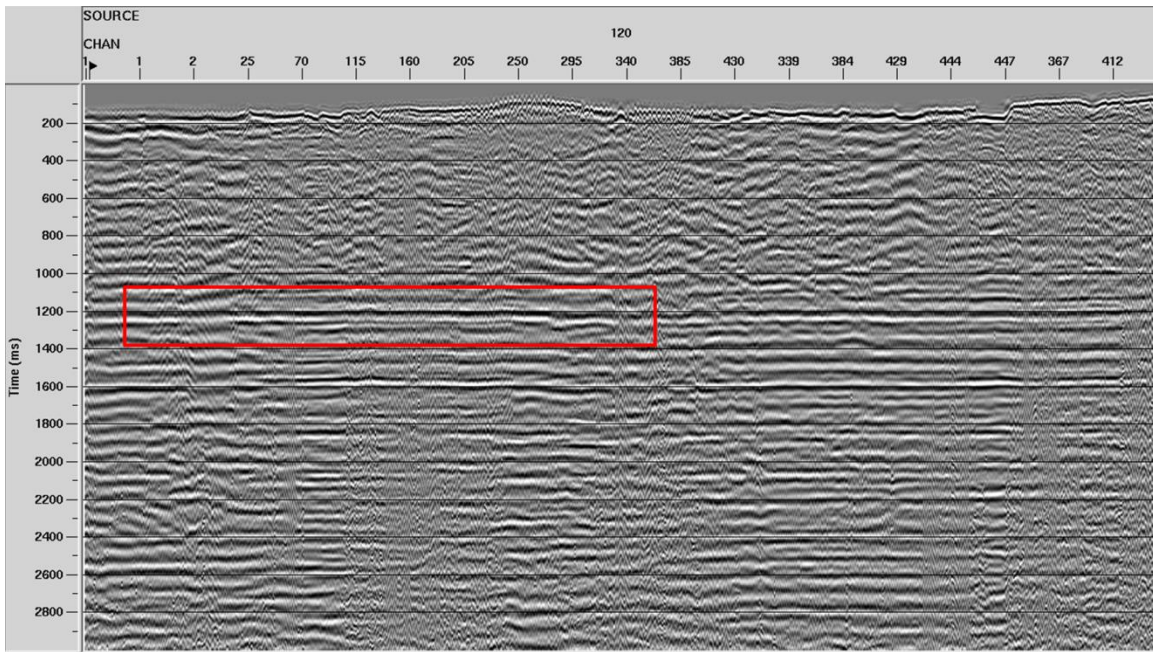
FIG. 9. Stacked section after tomostatics. The structure at 1200ms (red box) has been resolved and the continuity of the event has improved.
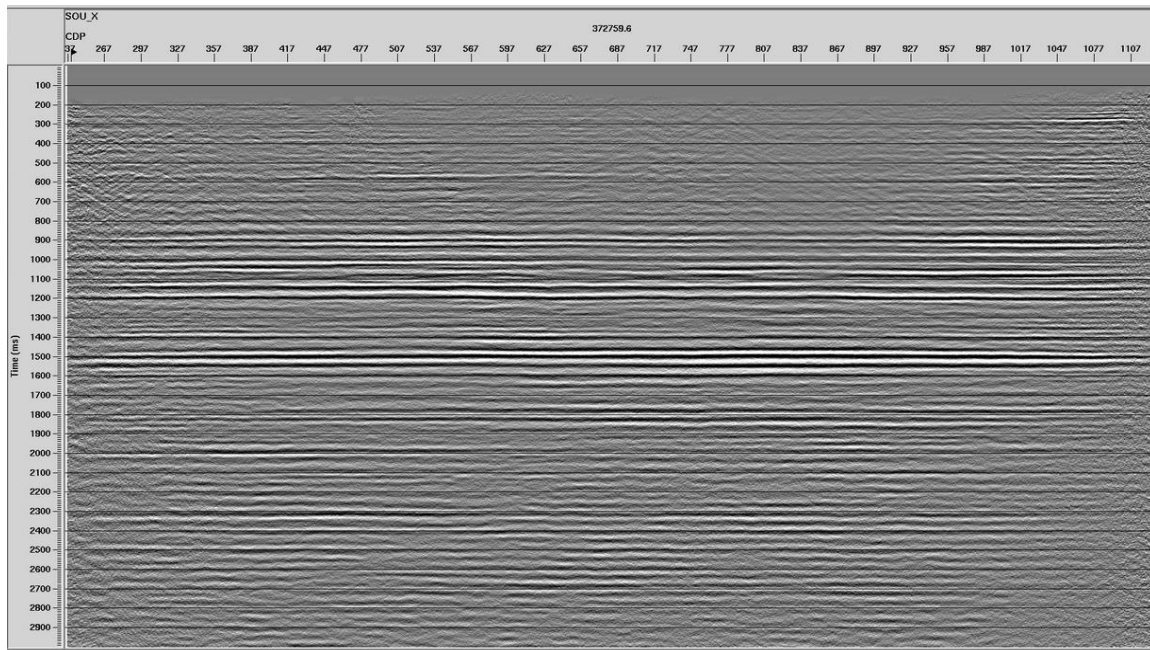
FIG. 10. Stack section with complete processing flow (Isaac and Margrave, 2011).

Figure 10 above is the final processed data by Helen Isaac and Gary Margrave 2011.

CONCLUSIONS AND DISCUSSIONS

Turning-ray tomography is a viable technique for statics correction as observed on Hussar data. In areas where there is an absence of a smooth refractor, tomostatics will produce better results compared with conventional refraction statics. The constrained damped SIRT method conditions the inversion and speeds up the convergence rate. One benefit of turning-ray tomography is that it makes no assumptions of the presence of reflectors, however due to the fact that it makes use of first arrivals, there is an inherent smoothing which increases as rays are traced into deeper sections in the model. The effect of this is a limitation on the resolution of the velocity model. The velocity model from turning-ray tomography can be used in depth conversion, wave equation datuming, prestack depth migration and as a starting model for full waveform inversion. Our results show that tomostatics improved reflectors continuity and corrected the structure of events. The final velocity model from tomography is also comparable to well logs velocities in the area.

ACKNOWLEDGEMENTS

REFERENCES

Bell, L., Lara, R., William, Gray, W.C., 1994 ; Application of turning-ray tomography to the offshore Mississippi Delta, SEG expanded abstracts **64**, 1509-1512.

Dennis, J.E., Schnabel, R.B., 1983; Numerical methods for unconstrained optimization and nonlinear equations, SIAM.

Isaac, J. H., Margrave, G. F., 2011; Hurrah for Hussar! Comparisons of stacked data, CREWES Research Report, **23**.

Jones, I., F., 2009; Velocity model building, EAGE Education Days.

Langan R.T., Lerche I., Cutler R.T., Bishop T.N., Spera N.J., 1984; Seismic tomography; The accurate and efficient tracing of rays through heterogeneous media, SEG Technical Program Extended Abstracts, 713-715.

Lo, T.W., Inderwiesen, P., 1994; Fundamentals of Seismic Tomography, SEG geophysical monograph series, N.6.

Pratt, R.G., Shipp, M., 1999; Seismic waveform inversion in the frequency domain-II: Fault delineation in sediments using crosshole data, Geophysics **64,** 901-913**.**

Promax, 1997; A reference guide for the Promax geophysical processing software, Landmark graphics corporation.

Stefani, J. P., 1993; Possibilities and Limitations of Turning Ray Tomography: A Synthetics Study, SEG Annual Meeting Extended Abstracts **63**, 610-612.

Stefani, J.P., 1995; Turning-ray tomography, Geophysics 60, 1917-1929.

Woodward, M.J., 1992; Wave-equation tomography, Geophysics **57**, 15-26.

Yilmaz, OZ., 2001; Seismic data analysis; Investigation in geophysics, **1.**

Zhu, X., Sixta, D. P., Angstman, B. G., 1992; Tomostatics: Tuning-ray Tomography + Static Corrections, The Leading Edge **11**, no. 12, 15-23.

Zhu, X., 2002; Velocity imaging through complex near-surface structures by Tomography, **64**[th] EAGE conference & Exhibition.

APPENDIX A

The two-point problem (Langan et al, 1984).

To find the ray-path between two points fixed on the surface using the shooting technique, a source sends out rays, spaced at equal increments of angle $\Delta\theta$. This fan of rays brackets all the receivers at the surface. The raypath to a given receiver is interpolated using equation A-1.

$$\theta_{new} = \theta_1 + (X_{revr} - X_1)\Delta\theta/\Delta X,$$

(A-1)

where θ_1 is the take-off angle for a ray in the fan on one side of the target receiver $X_{revr} - X_1$ is the distance between the target receiver and the surface position of the ray corresponding to θ_1, ΔX is the distance between the two rays which bracket the receiver, and θ_{new} is the take-off angle for the interpolated ray. Interpolation is repeated until the ray is close to the target receiver.